

Using the Backward Probability Method in contaminant source identification with a finite-duration source loading in a river

Hossein Khoshgou

Tarbiat Modares University

Seyed Ali Akbar Salehi Neyshabouri (✉ salehi@modares.ac.ir)

Tarbiat Modares University

Research Article

Keywords: Pollution source identification, Backward Probability Method, Adjoint Model, Finite-duration loading

Posted Date: June 15th, 2021

DOI: <https://doi.org/10.21203/rs.3.rs-203053/v1>

License:  This work is licensed under a Creative Commons Attribution 4.0 International License.

[Read Full License](#)

Version of Record: A version of this preprint was published at Environmental Science and Pollution Research on August 27th, 2021. See the published version at <https://doi.org/10.1007/s11356-021-15372-6>.

1 Using the Backward Probability Method in contaminant source identification with a 2 finite-duration source loading in a river

3 Hossein Khoshgou¹, Seyed Ali Akbar Salehi Neyshabouri²

4 1) h.khoshgou@modares.ac.ir (H. Khoshgou) M.Sc. Student of Water Resource Engineering and
5 Management, Department of Civil and Environmental Engineering, Tarbiat Modares University,
6 Tehran, Iran

7 2) Salehi@modares.ac.ir (S.A.A.S. Neyshabouri) Faculty of Civil and Environmental Engineering and
8 Water Engineering Research Center, Tarbiat Modares University, Tehran, Iran

9 Abstract

10 Violation of industries in discharging their effluents into rivers leads to river pollution, which
11 endangers the environment and human health. Appropriate tools are needed to deal with violations
12 and protect rivers. The Backward Probability Method (BPM) is one of the most recommended tools
13 identifying the release time and location of the pollutant source. However, the BPM generally was
14 developed for groundwater and spill injection. Since most industries inject their effluents with a
15 constant rate for a finite-duration, the use of prevailing models will have some errors. In this study, a
16 numerical model was developed that could simulate a source with either a finite-duration or spill
17 injection. This model is verified for two hypothetical cases and one real case. The results show that
18 the model can accurately identify the release time and location of the pollutant source.

19 **Keywords:** Pollution source identification, Backward Probability Method, Adjoint Model, Fintie-
20 duration loading

21 1. Introduction

22 Water is one of the most important and fundamental factors for living organisms. Surface water
23 resources, because of their availability and easy extraction, are widely used in industry, agriculture,
24 and municipal services. Surface water plays a prominent role in human societies (Cheng and Jia,
25 2010; Jing et al., 2020; Lu et al., 2015; Mazaheri et al., 2015; Rasheed et al., 2019; Saha et al., 2017).
26 Increasing the rate of using surface water resources led to increasing pollution of these resources and
27 scarcity of them (Amiri et al., 2019). Scarcity in water resources affects human lives and threatens
28 economic and social development (Duan et al., 2016; Jing et al., 2020). Therefore, protecting surface
29 water resources has become a global and security issue (Mekonnen and Hoekstra, 2018).

30 Environmental contaminant transport problems are broadly categorized into two subgroups, source-
31 based and receptor-based problems. In source-based problems, information about the source is
32 available, and the goal is to determine the concentration downgradient from the source (Neupauer and
33 Wilson, 1999). In order to respond to these problems, researchers use the solution of the transport
34 model (forward model) in which the advection-dispersion equation (ADE) is the base for analysis
35 (FISCHER et al., 1979; Runkel, 1996; Van Genuchten, 1981). In receptor-based problems,
36 contaminants are observed at monitoring points. In these cases, the main point is identifying source
37 location, release time, and injected mass. Researchers (Boano et al., 2007; Ghane et al., 2016;
38 Neupauer and Wilson, 1999; Tong and Deng, 2015) have used the inverse methods. In order to
39 respond to these problems. The approaches that are used in the inverse methods can be classified into
40 three categories: simulation-optimization approach, mathematical approach, and probabilistic
41 approach (Mazaheri et al., 2015).

42 The simulation-optimization approaches use a combination of optimization algorithms and the
43 forward model to solve the inverse problem. This method, despite its simple formulation, requires
44 high computational power. Alapati and Kabala (2000) used the least-squares method without any
45 regularization methods in order to reconstruct the released mass in groundwater aquifers.
46 Mahinthakumar and Sayeed (2005) claimed that combination methods have a better performance than
47 basic optimization, in which the goal is finding the relative minimum. They combined the genetic
48 algorithm with the basic optimizations in order to identify the source location. Xing et al. (2019)
49 proposed an ensemble surrogate model to identifying groundwater contaminant sources. This model
50 was following three individual surrogate models: kriging, radial basis function, and Monte Carlo
51 method. They could effectively identify not only conservative contaminants source but also
52 contaminants containing chemical reaction.

53 Mathematical approaches solve inverse problems in a direct manner and reduce computational costs.
54 However, complexity is considered a disadvantage of these approaches. Skaggs and Kabala (1994)
55 applied a mathematical method to calculate the release rate of pollutant sources; actually, they solved
56 the Fredholm integral equation. Thus, they used the Tikhonov regularization technique in a one-
57 dimensional domain to solve the inverse form of the ADE for groundwater. Milnes and Perrochet
58 (2007) used the concepts of transfer functions theory to find the location of pollutant sources in
59 groundwater aquifers. They could simulate this phenomenon as an inverse problem by using
60 concentration at the detection point. They showed that in the inverse solution, concentration contours
61 start to gather until these contours become a point that represents source location. Mazaheri et al.
62 (2015) tried to determine the release rate of pollutant sources in the river with non-steady non-uniform
63 flow conditions. They tried to resolve the problem of ill-posed equations by using the least square, the
64 Green's function, and the Tikhonov regularization method.

65 Probabilistic approaches use probabilistic distributions, and one of the important advantages of this
66 approach is small simulations and computations (Amiri et al., 2019). Liu (1995) established a
67 continuous inverse model that could identify the location of spill-releasing pollutants into
68 groundwater aquifers. In order to produce a probability density function (PDF), he used Laplace
69 transformations and inversed the flow velocity. Neupauer and Wilson (1999) tried to use the adjoint
70 method to solve the inverse ADE and produced a PDF. They verified their model using the model that
71 Liu (1995) presented. Neupauer and Wilson (2001) enhanced their method and showed that the
72 adjoint method could be used for multi-dimensional problems. They showed how the numerical
73 methods could be combined with the adjoint method in order to identify the release time and source
74 (Neupauer and Wilson 2004). Cheng and Jia (2010) were one of the first to try to identify the release
75 time and the source location in a river. They used the adjoint method under steady non-uniform flow
76 conditions; also, they assumed that the pollutant source is an instantaneous point source of a
77 contaminant. Ghane et al. (2016) realized the release time and the source location in a river using the
78 adjoint method by assuming one dimensional, steady, non-uniform flow conditions and an
79 instantaneous point of source contaminant. They used a hypothetical example and real river
80 conditions in order to verify their backward model. Jing et al. (2020) tried to obtain the pollutant
81 release mass in a river by using the adjoint method. They assumed that the pollutant source is a finite-
82 duration source, not instantaneous; their model was established for one-dimensional, steady non-
83 uniform flow conditions. They verified their model using two hypothetical examples and a real case
84 study.

85 Rivers are known as the main source of water for industry, irrigation, and domestic use. Therefore,
86 they must be constantly monitored for quality; In this case, identifying the source of the pollutant in
87 the rivers is important. Traditional pollutant source identification methods require a lot of data

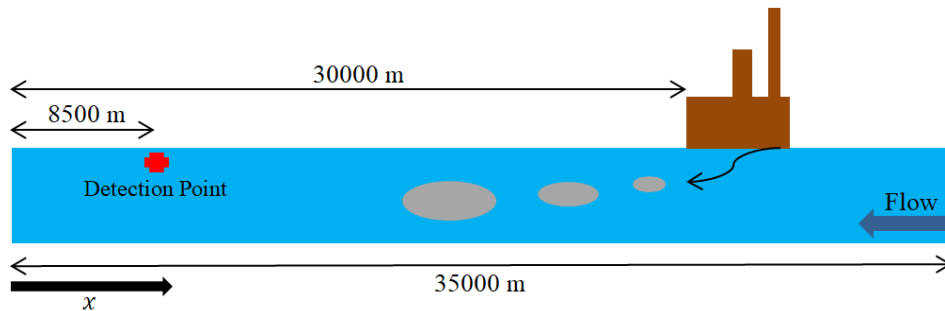
88 monitoring, including water quality, topographic and hydrological data, while numerical models of
 89 water quality modeling can be more efficient. The backward probability method as a numerical model
 90 can identify contaminant sources with limited data. In previous researches, the backward probability
 91 method is used for source identification in groundwater with an instantaneous point source. It is clear
 92 that many industries discharge their pollutants into the river in a step-loading manner. Therefore, to
 93 identify the industries that violate, it is necessary to develop a numerical model appropriate to this
 94 type of injection. Furthermore, the instantaneous and finite-duration injection should be discriminated.
 95 In this study, the adjoint method is applied for a source with a finite-duration injection, and the adjoint
 96 equations for steady uniform flow conditions and conservative pollutants are derived. The proposed
 97 model is validated by hypothetical and experimental examples.

98 **2. Study Area**

99 In order to verify the proposed model, a hypothetical problem and a real case are considered.

100 **2.1 Hypothetical Area**

101 In the hypothetical case, a hydrodynamically acceptable example should be defined. In this case, river
 102 width, flow velocity, roughness coefficient, and river slope were assumed; with these assumptions, the
 103 water depth and dispersion coefficient were calculated using Manning's equation and Fisher's equation
 104 (Hessel et al., 2003), respectively. Suppose that there is a factory upstream of a straight river. This
 105 factory, which is located 21500 m upstream of the monitoring point, discharged its sewage
 106 continuously in the river for a finite duration. Figure 1 shows the factory and the monitoring point
 107 location in the river. Table 1 lists the flow and transport properties of this example.



108

109 **Figure 1. Stright river geometry for case 1**

110

111

Table 1. Flow and transport properties in case 1

Parameter	Assumed values
Flow velocity (U)	1 m/s
Dispersion coefficient (D)	24 m ² /s
River width (b)	10 m
Water depth (y)	1 m
Initial concentration after mixing (C ₀)	50 kg/m ³
Discharge start time (t ₁)	0
Discharge completion time (t ₂)	1 hr

112

113

114 2.2 Chicago Waterway Area

115 Jackson and Lageman (2013) did a field trace experiment in which Rhodamine WT (RWT) dye was
116 injected for a finite-duration source estimation to the Chicago Sanitary and Ship Canal (Figure 2). In
117 this canal, six stations measured the dye concentration, two of which, fluorometer FL291 located 9930
118 m downstream of the source and FL293 located 7033 m downstream of the source, are used in this
119 study. The US Geological Survey collected the data. Hydrodynamic parameters used in the proposed
120 model are the calibration results of Zhu et al. (2017). More information can be found in Jackson and
121 Lageman (2013) and Zhu et al. (2017). Table 2 summarizes the field tracer experiment information.

122

3. Table 2. Flow and transport properties in Case 2

Parameter	Assumed values
Flow velocity (U)	0.14 m/s
Dispersion coefficient (D)	4 m ² /s
River width (b)	49 m
Water depth (y)	8 m
Initial concentration after mixing (C ₀)	10 μg/L
Discharge start time (t ₁)	December 2, 2009, at 19:51
Discharge completion time (t ₂)	December 3, 2009, at 04:47

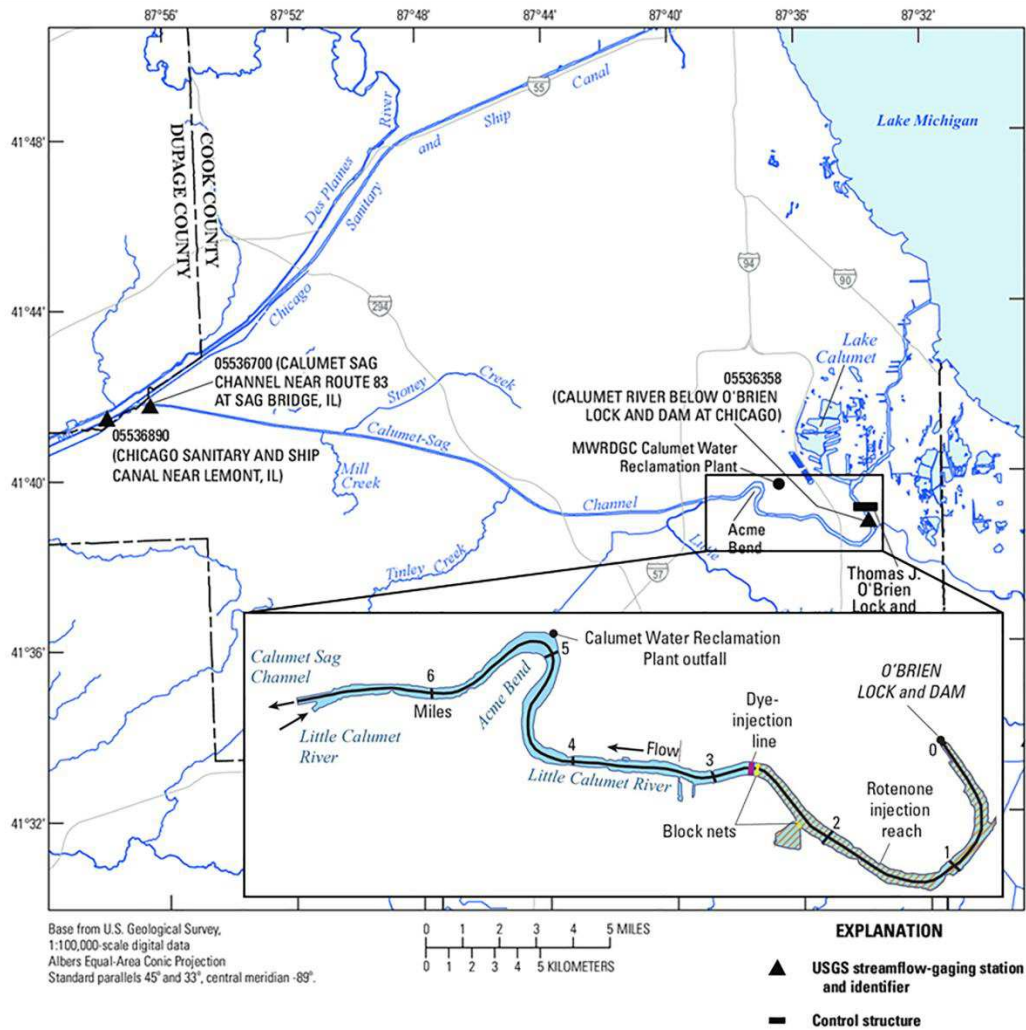


Figure 2. Map of Chicago waterway area

4. Methodology and Methods

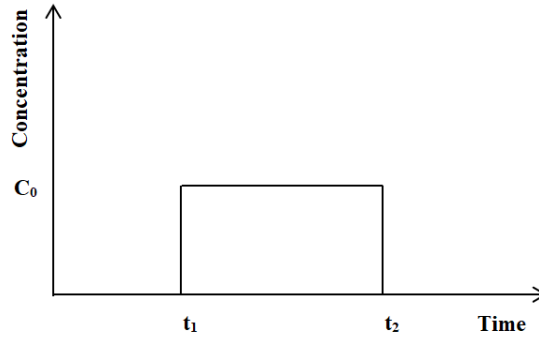
In this section, the forward model and the backward model are described. The prerequisite of solving the backward model is the forward model results. It was stated that the ADE was the base equation in the forward model. In order to solve the ADE, hydrodynamic conditions must be known; thus, a hydrodynamic model is used. Series of inputs and outputs derived from the hydrodynamic model are used in the ADE. The forward model results are used as inputs to the backward model to find the release time and source location. Furthermore, the identification process, the numerical model, and the way that the proposed model was verified are described.

4.1 Forward model

The basic governing equation of contaminant transport is the ADE that is shown as Eq. (1). This equation is for one dimensional, steady, and uniform flow conditions (Chapra, 1997):

$$\frac{\partial C}{\partial t} = D \frac{\partial^2 C}{\partial x^2} - U \frac{\partial C}{\partial x} + S + KC \quad (1)$$

137 where C is the concentration, D is the longitudinal dispersion coefficient, U is the flow velocity, S is
 138 the source term, K is the first-order decay rate coefficient, t is the forward time, and x is the
 139 longitudinal coordinate. The source term defines the characteristics of the source and shows how
 140 pollutants discharge into the river. In this study, identifying the source of the pollutants in the river
 141 with a finite duration of injection (step loading, Figure 3) is the main idea. Therefore, the source term
 142 can be defined, as shown in Eq. (2):



143

144

Figure 3. Step loading with a finite duration

$$S = C_0 \delta(x - x_s) [H(t - t_1) - H(t - t_2)] \quad (2)$$

145 where C_0 is the initial concentration at the source location, δ is the Delta Dirac Function, H is the
 146 Heaviside Function, t_1 is the time that pollutant injection starts, and t_2 is the time that pollutant
 147 injection stops. Considering a conservative solute ($K=0$), and the ADE and its initial and boundary
 148 conditions became as shown in Eq. (3) (Cheng and Jia, 2010).

$$\frac{\partial C}{\partial t} = D \frac{\partial^2 C}{\partial x^2} - U \frac{\partial C}{\partial x} + S$$

$$C(x, t) = 0 \quad \text{at} \quad x = \infty \quad (3)$$

$$\frac{\partial C}{\partial x} = 0 \quad \text{at} \quad x = 0$$

$$C(x, 0) = 0 \quad \text{at} \quad x \geq 0$$

$$S = C_0 \delta(x - x_s) [H(t - t_1) - H(t - t_2)] \quad (4)$$

149 The result of solving equation Eq. (3) is the concentration at time t and location x . Normalizing
 150 concentration by the total concentration entering the system defines the Forward Location Probability
 151 (FLP) from source to the detection point (Neupauer and Wilson, 1999). Equation Eq. (5) shows this
 152 expression:

$$f(x, t) = \frac{C(x, t)}{\int_0^\infty C(x, t) dt} \quad (5)$$

153 In this study, it is assumed to have a steady and uniform flow condition. Manning's equation and
 154 Fisher's equation are used in order to determine the hydrodynamic parameters (A, U, and D). Eq. (6)
 155 represents Manning's equation, and Eq. (7) represents Fisher's equation.

$$U = \frac{1}{n} R^{2/3} S^{1/2} \quad (6)$$

$$D = 0.011 \frac{U^2 B^2}{H U^*} \quad (7)$$

$$U^* = \sqrt{gHS} \quad (8)$$

156 where n is a Manning's roughness coefficient, R is the channel hydraulic radius, S is the channel
 157 slope, B is the average channel width, H is the average depth, and U^* is the shear velocity.

158 4.2 Backward model

159 The adjoint method is used in order to form the backward model. The adjoint of the ADE for the
 160 finite-duration of injection was developed by pursuing the steps that (Neupauer and Wilson, 1999)
 161 established. The performance measure, P, expresses the state of the system and is defined as Eq. (9):

$$P = \int_{x_1}^{x_2} \int_0^{\infty} h(\alpha, C) dt dx \quad (9)$$

162

163 where $h(\alpha, C)$ is a function of the state of the system, and α is a vector of system parameters ($U, D,$
 164 C_0). The marginal sensitivity is obtained by differentiating the performance measure with respect to
 165 one of the system parameters Eq. (10) shows marginal sensitivity in which differentiation is with
 166 respect to C_0 .

$$\frac{dP}{dC_0} = \int_{x_1}^{x_2} \int_0^{\infty} \left[\frac{\partial h(\alpha, C)}{\partial C_0} + \frac{h(\alpha, C)}{\partial C} \psi \right] dt dx \quad (10)$$

167

168 where dP/dC_0 is defined as a marginal sensitivity, $\psi = \partial C / \partial C_0$ is a state sensitivity that indicates the
 169 measure of the change in the state of the system. The state sensitivity in Eq. (10) is unknown; thus, in
 170 order to calculate the marginal sensitivity, ψ from Eq. (10) must be eliminated by using the adjoint
 171 method. The first step in utilizing the adjoint method is differentiating the ADE, and its initial and
 172 boundary conditions respect to the C_0 . Differentiating Eq. (3) respect to the C_0 gives:

$$\begin{aligned} -\frac{\partial \psi}{\partial t} + D \frac{\partial^2 \psi}{\partial x^2} - U \frac{\partial \psi}{\partial x} + \frac{\partial S}{\partial C_0} &= 0 \\ \psi(x, t) &= 0 \quad \text{at} \quad x = \infty \\ \frac{\partial \psi}{\partial x} &= 0 \quad \text{at} \quad x = 0 \\ \psi(x, 0) &= 0 \quad \text{at} \quad x \geq 0 \end{aligned} \quad (11)$$

173 The next step is obtaining to an equation similar to the ADE in which ψ^* , an arbitrary function, is the
 174 main variable. It will be shown that ψ^* is the adjoint state. Therefore, the inner product of the adjoint
 175 state and each term in Eq. (11) is taken after defining the inner product of two functions.

$$\int_0^T \int_{x_1}^{x_2} \left[-\psi^* \frac{\partial \psi}{\partial t} + \psi^* D \frac{\partial^2 \psi}{\partial x^2} - \psi^* U \frac{\partial \psi}{\partial x} + \psi^* \frac{\partial S}{\partial C_0} \right] dx dt = 0 \quad (12)$$

176 where T is the final time (detection time), x_1 , and x_2 are the downstream and the upstream boundaries,
177 respectively. A similar form of the ADE for ψ^* is obtained by manipulating each term in Eq. (12).

$$\int_0^T \int_{x_1}^{x_2} -\psi^* \frac{\partial \psi}{\partial t} dx dt = \int_0^T \int_{x_1}^{x_2} -\frac{\partial}{\partial t} (\psi^* \psi) + \psi \frac{\partial \psi^*}{\partial t} dx dt \quad (13)$$

$$\begin{aligned} \int_0^T \int_{x_1}^{x_2} \psi^* D \frac{\partial^2 \psi}{\partial x^2} dx dt \\ = \int_0^T \int_{x_1}^{x_2} D \frac{\partial}{\partial x} \left(\psi^* \frac{\partial \psi}{\partial x} \right) - D \frac{\partial \psi}{\partial x} \frac{\partial \psi^*}{\partial x} dx dt \end{aligned} \quad (14)$$

$$\begin{aligned} \int_0^T \int_{x_1}^{x_2} -D \frac{\partial \psi}{\partial x} \frac{\partial \psi^*}{\partial x} dx dt \\ = \int_0^T \int_{x_1}^{x_2} -D \frac{\partial}{\partial x} \left(\psi \frac{\partial \psi^*}{\partial x} \right) + \psi D \frac{\partial^2 \psi^*}{\partial x^2} dx dt \end{aligned} \quad (15)$$

$$\begin{aligned} \int_0^T \int_{x_1}^{x_2} -\psi^* U \frac{\partial \psi}{\partial x} dx dt \\ = \int_0^T \int_{x_1}^{x_2} -U \frac{\partial}{\partial x} (\psi^* \psi) + U \psi \frac{\partial \psi^*}{\partial x} dx dt \end{aligned} \quad (16)$$

178

179 Substituting Eq. (13), Eq. (14), Eq. (15), and Eq. (16) into Eq. (12) gives:

$$\begin{aligned} \int_0^T \int_{x_1}^{x_2} \left[-\frac{\partial}{\partial t} (\psi^* \psi) + \psi \frac{\partial \psi^*}{\partial t} + D \frac{\partial}{\partial x} \left(\psi^* \frac{\partial \psi}{\partial x} \right) - D \frac{\partial}{\partial x} \left(\psi \frac{\partial \psi^*}{\partial x} \right) \right. \\ \left. + \psi D \frac{\partial^2 \psi^*}{\partial x^2} - U \frac{\partial}{\partial x} (\psi^* \psi) + U \psi \frac{\partial \psi^*}{\partial x} \right. \\ \left. + \psi^* \frac{\partial S}{\partial C_0} \right] dx dt = 0 \end{aligned} \quad (17)$$

180 The left side of Eq. (17) is equal to zero; thus, it can be added to the right side of Eq. (10) without a
181 change in results. Equation Eq. (18) shows the new expression of the marginal sensitivity. It is
182 obtained by rearranging terms after adding the left side of Eq. (17) to the right side of Eq. (10).

$$\begin{aligned} \frac{dP}{dC_0} = \int_0^T \int_{x_1}^{x_2} \left\{ \frac{\partial h(\alpha, C)}{\partial C_0} + \psi \left[\frac{h(\alpha, C)}{\partial C} + \frac{\partial \psi^*}{\partial t} + D \frac{\partial^2 \psi^*}{\partial x^2} + U \frac{\partial \psi^*}{\partial x} \right] \right. \\ \left. + \frac{\partial}{\partial x} \left[D \psi^* \frac{\partial \psi}{\partial x} - D \psi \frac{\partial \psi^*}{\partial x} - U \psi^* \psi \right] - \frac{\partial}{\partial t} (\psi^* \psi) \right. \\ \left. + \psi^* \frac{\partial S}{\partial C_0} \right\} dx dt \end{aligned} \quad (18)$$

183 The current goal is to eliminate ψ from Eq. (18). Therefore, it can be assumed that $\frac{\partial h(\alpha, C)}{\partial C_0} = 0$,
184 because the system parameters (e.g., U , and D) are independent of C_0 . The coefficient of ψ in the
185 second term of integration in Eq. (18) is equal to zero (the adjoint equation). The third and fourth
186 terms are divergence terms and represent initial and boundary conditions for the adjoint equation after
187 integration. These assumptions are shown in Eq. (19), Eq. (20), and Eq. (21).

$$\frac{h(\alpha, C)}{\partial C} + \frac{\partial \psi^*}{\partial t} + D \frac{\partial^2 \psi^*}{\partial x^2} + U \frac{\partial \psi^*}{\partial x} = 0 \quad (19)$$

$$\int_0^T \int_{x_1}^{x_2} \frac{\partial}{\partial x} \left[D \psi^* \frac{\partial \psi}{\partial x} - D \psi \frac{\partial \psi^*}{\partial x} - U \psi^* \psi \right] dx dt = 0 \quad (20)$$

$$\int_0^T \left[D \psi^* \frac{\partial \psi}{\partial x} - D \psi \frac{\partial \psi^*}{\partial x} - U \psi^* \psi \right] \Big|_{x_1}^{x_2} dt = 0$$

188 Substituting conditions that represented in Eq. (9) into Eq. (17) gives:

$$D \psi^* \frac{\partial \psi}{\partial x} \Big|_{x=\infty} + D \psi \frac{\partial \psi^*}{\partial x} \Big|_{x=0} + U \psi^* \psi \Big|_{x=0} = 0 \quad (21)$$

189 As previously indicated, the adjoint state, ψ^* , is an arbitrary function and can be defined to
 190 eliminate ψ . Therefore, the initial and boundary conditions for the adjoint equation are shown in Eq.
 191 (22) and Eq. (23):

$$\psi^*(x, t) = 0 \quad \text{at } x = \infty \quad (22)$$

$$D \frac{\partial \psi^*}{\partial x} + U \psi^* = 0 \quad \text{at } x = 0$$

$$\int_{x_1}^{x_2} \int_0^T -\frac{\partial}{\partial t} (\psi^* \psi) dt dx = 0$$

$$\int_{x_1}^{x_2} (\psi^* \psi) \Big|_0^T dx = 0 \quad (23)$$

$$\psi^*(x, T) = 0 \quad \text{at } x \geq 0$$

192 The final time in the forward model, T , is determined arbitrarily, and $t \leq t_d$ is essential; thus, the
 193 detection time can be determined as the final time. In the backward model, backward time is used, τ ,
 194 which defined as $\tau = T - t = t_d - t$. The definition of the function of the state, $h(\alpha, C)$, is related to
 195 the performance measure. When the performance measure was considered as a concentration at a
 196 known time and location, i.e., the detection point, the function of the state should be defined in a way
 197 that the integration over the time and space domain results in the measured concentration at the
 198 detection point. Therefore, the function of the state can be defined as Eq. (24). $h(\alpha, C)/\partial C$ is a Frechet
 199 derivative (Saaty, 1981) of $h(\alpha, C)$ with respect to the C . take the derivative of both sides of Eq. (24)
 200 gives Eq. (25). Eq. (26) represents the marginal sensitivity. Eq. (27) shows the adjoint equation and its
 201 initial and boundary conditions.

$$h(\alpha, C) = C(x, t) \delta(x - x_d) \delta(t - t_d) \quad (24)$$

$$\frac{h(\alpha, C)}{\partial C} = \delta(x - x_d) \delta(t - t_d) \quad (25)$$

$$\begin{aligned}\frac{dP}{dC_0} &= \int_0^T \int_{x_1}^{x_2} \psi^* \frac{\partial S}{\partial C_0} dxdt \\ &= \int_0^T \int_{x_1}^{x_2} \psi^* \delta(x - x_s) [H(t - t_1) - H(t - t_2)] dxdt\end{aligned}\quad (26)$$

$$\frac{\partial \psi^*}{\partial \tau} + D \frac{\partial^2 \psi^*}{\partial x^2} + U \frac{\partial \psi^*}{\partial x} = -\delta(x - x_d) \delta(t - t_d)$$

$$\psi^*(x, \tau) = 0 \quad \text{at} \quad x = \infty \quad (27)$$

$$D \frac{\partial \psi^*}{\partial x} + U \psi^* = 0 \quad \text{at} \quad x = 0$$

$$\psi^*(x, 0) = 0 \quad \text{at} \quad x \geq 0$$

202

203 Results of Eq. (27) are the adjoint state at every point in the time and space domain. Using these
 204 results in Eq. (26) gives the marginal sensitivity. Eq. (28) shows Backward Location Probability
 205 (BLP).

$$f(x, \tau) = \frac{1}{(t_2 - t_1)} \frac{dP}{dC_0} \quad (28)$$

206

4.3 Identification process

207 The FLP demonstrates the probability of the existence of a contaminant that has been released from
 208 the source at a particular location (detection point) after passing the specific time. However, the BLP
 209 determines the prior location of a contaminant that has been observed at the detection point (Neupauer
 210 and Wilson, 2001). Based on the backward probability method, BLP and FLP density functions are
 211 equal only at the source location (Wagner et al., 2015). The Root Mean Square Error (RMSE) have
 212 been used to compare the BLP and FLP density functions (Cheng and Jia, 2010; Ghane et al., 2016),
 213 which Eq. (29) shows:

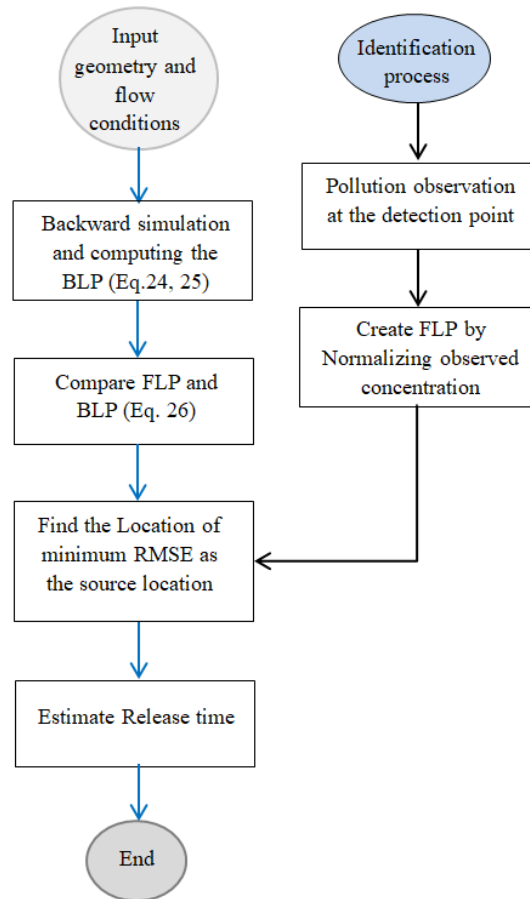
$$RMSE = \sqrt{\frac{\sum_{i=1}^n (FLP - BLP)^2}{n}} \quad (29)$$

214 where n is the number of data entry points to be compared, the source location will be identified when
 215 the RMSE is minimized. Figure 4 shows the overall identification process.

216

4.4 Numerical Modeling

217 A numerical model has been developed to compute the forward and backward probabilities. This
 218 numerical model is based on the Finite Volume Method with the upwind and fully implicit scheme in
 219 space and time. The applied numerical model can solve Eq. (3) and Eq. (27). The Delta Dirac
 220 Function in Eq. (27) and Eq. (3) estimated and applied using the scheme proposed by Neupauer and
 221 Wilson (2004).



222

223

Figure 4. Flow chart of the identification process.

224

5. Results and discussion

225

The proposed model is verified for a hypothetical case and a real case. Also, it is expected that this model could simulate an instantaneous source since, in the step loading source, when the difference between the time that source starts and stops to inject contaminant becomes zero, $t_1-t_2=0$, the source becomes an instantaneous source. Therefore, this ability was verified by using a hypothetical case.

228

5.1 Finite-duration source (Case 1)

229

230

After injection, the monitoring point records concentration over time (Figure 5a), and the numerical model uses Eq. (5) to produce the FLP. The proposed model calculates the BLP for every possible source location and compares it with FLP (Figure 4b). However, the minimum RMSE between BLP and FLP shows source location. In this case, the model determined $x = 30000\text{ m}$ as a contaminant source location since it has the minimum $\text{RMSE} = 1.89 \times 10^{-5}$. Figure 5a shows that 6.475 h after injection, peak concentration reaches to the monitoring point. The peak concentration was considered as the presence of a contaminant at a specific location (Neupauer and Wilson, 1999). Figure 5b shows the best match between BLP and FLP, and the highest probability for the release time from the detected source location is 6.475 h before observing contaminants in the monitoring point. As it is clear, the model could identify the release time and location with the least error.

231

232

233

234

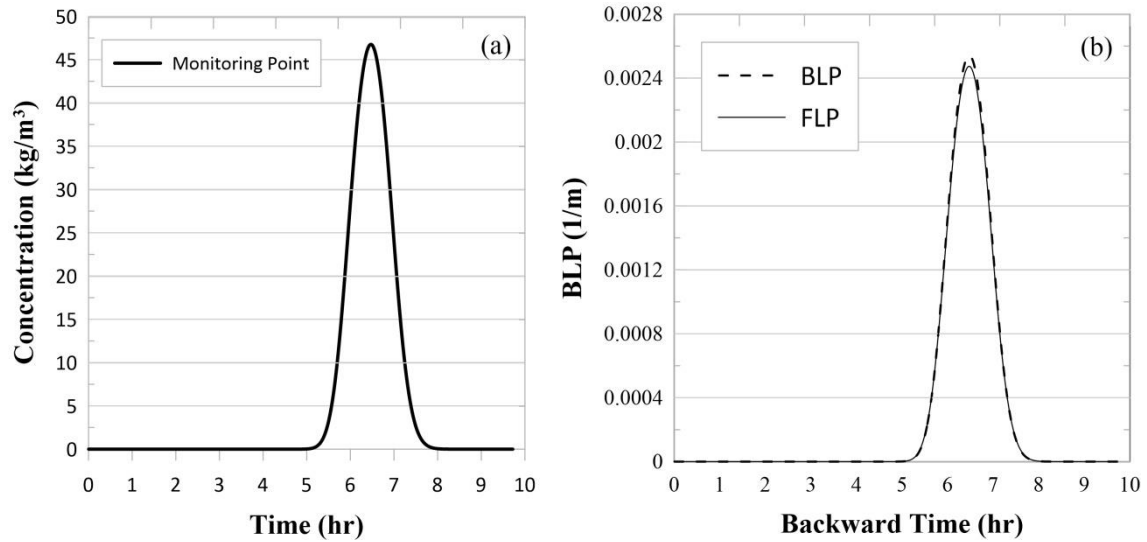
235

236

237

238

239

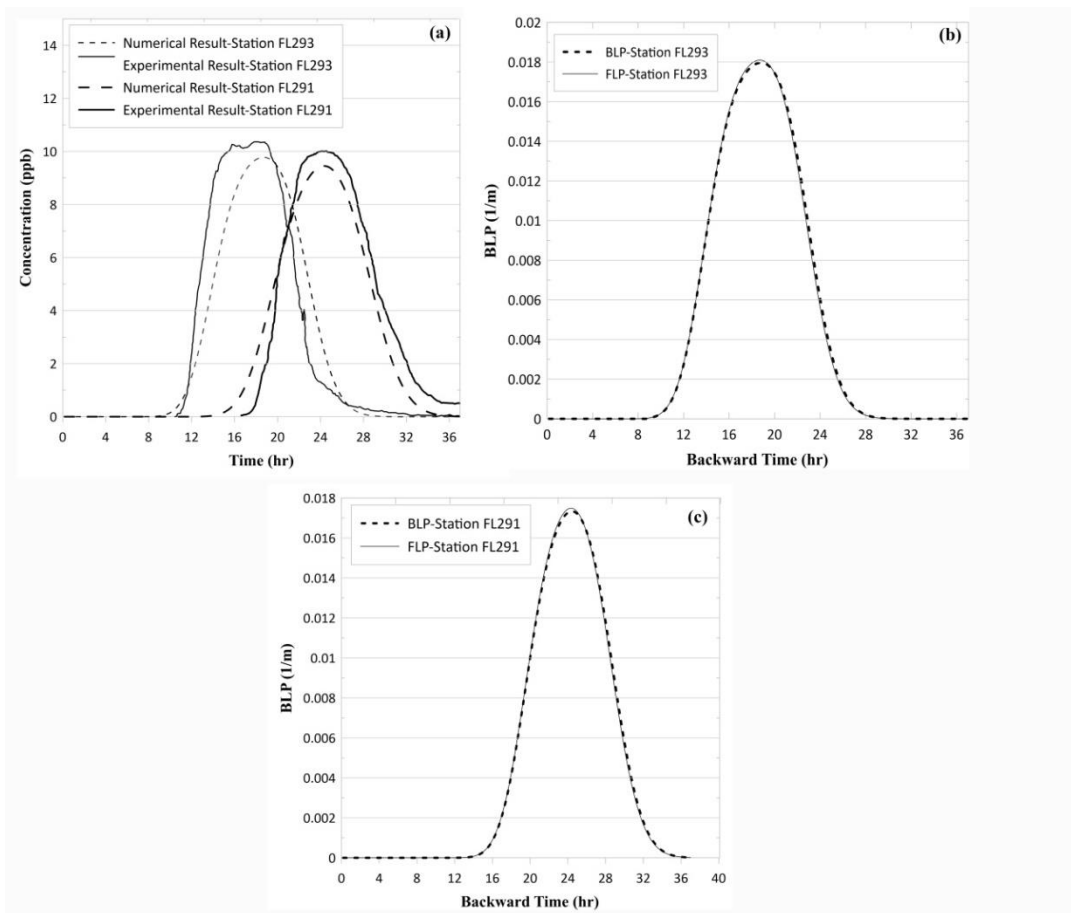


240

241 **Figure 5. a) Concentration time series at monitoring point, b) Comparison between BLP and FLP**

242 **5.2 Field tracer experiments (Case 2)**

243 Figure 6a shows a comparison between measured concentrations at two stations and the numerical
 244 results. As shown, the peak arrival time in both numerical and measured concentrations for
 245 FL291 station is 24.3 hours after injection. The peak arrival time for FL293 station in the numerical
 246 model is 18.6 hours after injection, and in the field tracer experiment is 17.67 hours. Figure 6b and 6c
 247 show a best match between the FLP and BLP. The best match with minimum RMSE shows that the
 248 model can identify the source location in both tests. The source location that have minimum RMSE
 249 (0.002 for FL291 and 0.0024 for FL293) based on the observations at stations FL291 and FL293.

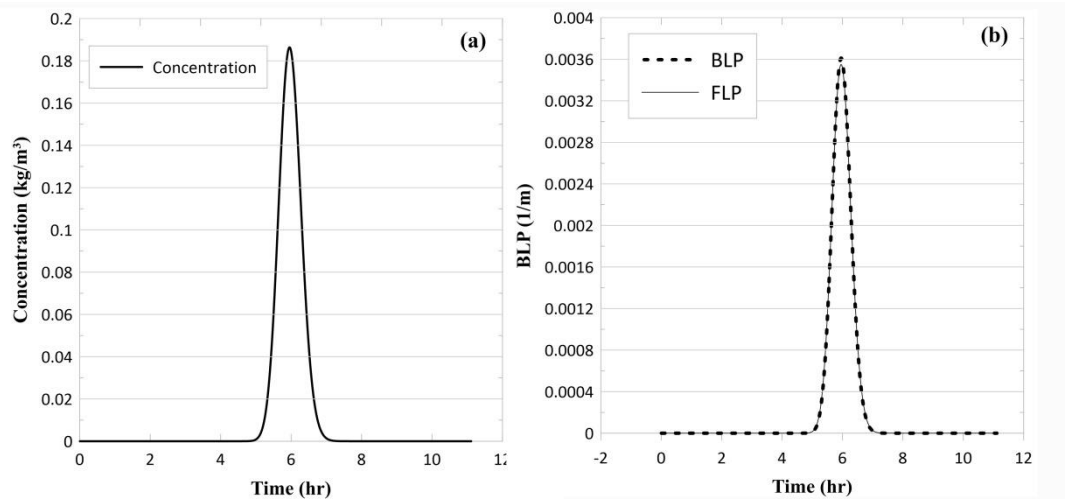


250

251 **Figure 6. a) Comparison of concentration between numerical model and field tracer experiment at two**
 252 **stations b) Comparison between the BLP and FLP at station FL293, and c) Comparison between the BLP**
 253 **and FLP at station FL291**

254 5.3 Instantaneous source (case 3)

255 Case 3 is defined to show that the proposed model can identify the release time and location of the
 256 contaminant source when the injection happens as an instantaneous source. In Case 3, the hypothetical
 257 example that is represented in Case 1 is used. However, If the model is used for simulating an
 258 instantaneous source, the difference between the time that the source starts and stops injection must be
 259 zero, $t_2 - t_1 = 0$. Figure 7a shows the concentration time series at the monitoring point; based on the
 260 results in Figure 7a the FLP became accessible. The peak concentration reaches the monitoring point
 261 5.96 h after injection. Figure 7b shows the comparison between the FLP and BLP at the source
 262 location, which has the minimum RMSE (1.22×10^{-5}). Based on Figure 7b the highest probability
 263 for release time is 5.96 h before the injection.



264

265 **Figure 7. a) Concentration time series at the monitoring point for an instantaneous source b) Comparison**
 266 **between the FLP and the BLP**

267 The proposed model has been validated by the three examples. The results show that this model can
 268 properly identify source location and release time. Most of the previous studies simulate instantaneous
 269 injection. With this in mind, in the third example, the proposed model could simulate instantaneous
 270 injection and determine the release time and source location. Furthermore, a sensitivity analysis for
 271 hydrodynamic parameters was done, and the results indicated that the model could identify the release
 272 time and source location correctly, and changing hydrodynamic parameters does not significantly
 273 affect the results.

274 6. Conclusions

275 In this study, an adjoint method was developed for a finite-duration injection to a river in order to
 276 expand previous studies. The proposed model successfully simulated steady uniform flow conditions
 277 and conservative pollutants. The results showed that when conservative pollutants exist, a monitoring
 278 point is sufficient for determining the release time and source location. Furthermore, the model
 279 performance in a real case was examined, and it was concluded that the model works accurately. The
 280 maximum error for release time and source location, in some cases, was 6%. Also, this model can be
 281 used for large-scale rivers and instantaneous sources. The adjoint method identifies the source
 282 location and release time by simulating the backward model once which is a beneficial ability
 283 compared to other methods in the literature.

284 Acknowledgements

285 This research did not receive any specific grant from funding agencies in the public, commercial, or
 286 not-for-profit sectors.

287 Ethical Approval

288 This manuscript is our original, unpublished paper, which we did not submit to another journal before.

289 Consent to Participate and Publish

290 It is our great pleasure to submit to you my manuscript entitled “Using the Backward Probability
 291 Method in contaminant source identification with a finite-duration source loading in the river” to be
 292 published in your admired journal.

293 **Authors Contributions**

294 Hossein Khoshgou is an M.Sc. student, and this paper originated from his thesis, and Seyed Ali Akbar
295 Salehi Neyshabouri is his supervisor and corresponding author.

296 **Competing Interests**

297 The authors declare that they have no known competing financial interests or personal relationships
298 that could have appeared to influence the work reported in this paper.

299 **Availability of data and materials**

300 There is no availability for data and materials.

301 **References**

- 302 Alapati, S., Kabala, Z.J., 2000. Recovering the release history of a groundwater contaminant using a
303 non-linear least-squares method. *Hydrol. Process.* 14, 1003–1016.
304 [https://doi.org/10.1002/\(SICI\)1099-1085\(20000430\)14:6<1003::AID-HYP981>3.0.CO;2-W](https://doi.org/10.1002/(SICI)1099-1085(20000430)14:6<1003::AID-HYP981>3.0.CO;2-W)
- 305 Amiri, S., Mazaheri, M., Mohammad Vali Samani, J., 2019. Introducing a general framework for
306 pollution source identification in surface water resources (theory and application). *J. Environ.*
307 *Manage.* 248, 109281. <https://doi.org/10.1016/j.jenvman.2019.109281>
- 308 Boano, F., Packman, A.I., Cortis, A., Revelli, R., Ridolfi, L., 2007. A continuous time random walk
309 approach to the stream transport of solutes. *Water Resour. Res.* 43, 1–12.
310 <https://doi.org/10.1029/2007WR006062>
- 311 Chapra, S., 1997. *Surface water-quality modeling*. McGraw-Hill, New York.
- 312 Cheng, W.P., Jia, Y., 2010. Identification of contaminant point source in surface waters based on
313 backward location probability density function method. *Adv. Water Resour.* 33, 397–410.
314 <https://doi.org/10.1016/j.advwatres.2010.01.004>
- 315 Duan, W., He, B., Nover, D., Yang, G., Chen, W., Meng, H., Zou, S., Liu, C., 2016. Water quality
316 assessment and pollution source identification of the eastern poyang lake basin using
317 multivariate statistical methods. *Sustain.* 8, 1–15. <https://doi.org/10.3390/su8020133>
- 318 FISCHER, H.B., LIST, E.J., KOH, R.C.Y., IMBERGER, J., BROOKS, N.H., 1979. Concepts and
319 Definitions. *Mix. Inl. Coast. Waters* 1–29. <https://doi.org/10.1016/b978-0-08-051177-1.50005-2>
- 320 Fisher, B.H., 1975. Discussion of simple method for predicting dispersion in streams. *J. Envir. Engrg.*
321 *Div., ASCE*, 101(3), 453-455. <https://doi.org/10.1061/JEEGAV.0000360>
- 322 Ghane, A., Mazaheri, M., Mohammad Vali Samani, J., 2016. Location and release time identification
323 of pollution point source in river networks based on the Backward Probability Method. *J.*
324 *Environ. Manage.* 180, 164–171. <https://doi.org/10.1016/j.jenvman.2016.05.015>
- 325 Hessel, R., Jetten, V., Guanghui, Z., 2003. Estimating Manning's n for steep slopes. *Catena* 54, 77–
326 91. [https://doi.org/10.1016/S0341-8162\(03\)00058-4](https://doi.org/10.1016/S0341-8162(03)00058-4)
- 327 Jackson, P.R., Lageman, J.D., 2013. Real-time piscicide tracking using Rhodamine WT dye for
328 support of application, transport, and deactivation strategies in riverine environments. *Sci.*
329 *Investig. Rep.* 56. <https://doi.org/10.3133/sir20135211>
- 330 Jing, P., Yang, Z., Zhou, W., Huai, W., Lu, X., 2020. Inverse estimation of finite-duration source
331 release mass in river pollution accidents based on adjoint equation method. *Environ. Sci. Pollut.*

- 332 Res. 27, 14679–14689. <https://doi.org/10.1007/s11356-020-07841-1>
- 333 Liu, J., 1995. Travel time and location probabilities for groundwater contaminant source.
334 https://doi.org/http://www.ees.nmt.edu/outside/alumni/papers/1995t_liu_j.pdf
- 335 Lu, Y., Song, S., Wang, R., Liu, Z., Meng, J., Sweetman, A.J., Jenkins, A., Ferrier, R.C., Li, H., Luo,
336 W., Wang, T., 2015. Impacts of soil and water pollution on food safety and health risks in China.
337 *Environ. Int.* 77, 5–15. <https://doi.org/10.1016/j.envint.2014.12.010>
- 338 Mahinthakumar, G., Sayeed, M., 2005. Hybrid genetic algorithm - Local search methods for solving
339 groundwater source identification inverse problems. *J. Water Resour. Plan. Manag.* 131, 45–57.
340 [https://doi.org/10.1061/\(ASCE\)0733-9496\(2005\)131:1\(45\)](https://doi.org/10.1061/(ASCE)0733-9496(2005)131:1(45))
- 341 Mazaheri, M., Mohammad Vali Samani, J., Samani, H.M.V., 2015. Mathematical Model for Pollution
342 Source Identification in Rivers. *Environ. Forensics* 16, 310–321.
343 <https://doi.org/10.1080/15275922.2015.1059391>
- 344 Mekonnen, M.M., Hoekstra, A.Y., 2018. Global Anthropogenic Phosphorus Loads to Freshwater and
345 Associated Grey Water Footprints and Water Pollution Levels: A High-Resolution Global
346 Study. *Water Resour. Res.* 54, 345–358. <https://doi.org/10.1002/2017WR020448>
- 347 Milnes, E., Perrochet, P., 2007. Simultaneous identification of a single pollution point-source location
348 and contamination time under known flow field conditions. *Adv. Water Resour.* 30, 2439–2446.
349 <https://doi.org/10.1016/j.advwatres.2007.05.013>
- 350 Neupauer, R.M., Wilson, J.L., 2004. Numerical implementation of a backward probabilistic model of
351 ground water contamination. *Ground Water* 42, 175–189.
352 <https://doi.org/https://doi.org/10.1111/j.1745-6584.2004.tb02666.x>
- 353 Neupauer, R.M., Wilson, J.L., 2001. Adjoint-derived location and travel time probabilities for a
354 multidimensional groundwater system. *Water Resour. Res.* 37, 1657–1668.
355 <https://doi.org/http://dx.doi.org/10.1029/2000WR900388>; doi:10.102
- 356 Neupauer, R.M., Wilson, J.L., 1999. Adjoint method for obtaining backward-in-time location and
357 travel time probabilities of a conservative groundwater contaminant. *Water Resour. Res.* 35,
358 3389–3398. <https://doi.org/10.1029/1999WR900190>
- 359 Rasheed, T., Bilal, M., Nabeel, F., Adeel, M., Iqbal, H.M.N., 2019. Environmentally-related
360 contaminants of high concern: Potential sources and analytical modalities for detection,
361 quantification, and treatment. *Environ. Int.* 122, 52–66.
362 <https://doi.org/10.1016/j.envint.2018.11.038>
- 363 Runkel, R.L., 1996. Solution of the advection-dispersion equation: continuous load of finite duration.
364 *Environ. Eng.* 122, 830–832. [https://doi.org/https://doi.org/10.1061/\(ASCE\)0733-
365 9372\(1996\)122:9\(830\)](https://doi.org/https://doi.org/10.1061/(ASCE)0733-9372(1996)122:9(830))
- 366 Saha, N., Rahman, M.S., Ahmed, M.B., Zhou, J.L., Ngo, H.H., Guo, W., 2017. Industrial metal
367 pollution in water and probabilistic assessment of human health risk. *J. Environ. Manage.* 185,
368 70–78. <https://doi.org/10.1016/j.jenvman.2016.10.023>
- 369 Skaggs, T.H., Kabala, Z.J., 1994. Recovering the release history of a groundwater contaminant. *Water
370 Resour. Res.* 30, 71–79. <https://doi.org/10.1029/93WR02656>
- 371 Tong, Y., Deng, Z., 2015. Moment-Based Method for Identification of Pollution Source in Rivers. *J.
372 Environ. Eng. (United States)* 141. [https://doi.org/10.1061/\(ASCE\)EE.1943-7870.0000683](https://doi.org/10.1061/(ASCE)EE.1943-7870.0000683)
- 373 Van Genuchten, M.T., 1981. Analytical solutions for chemical transport with simultaneous
374 adsorption, zero-order production and first-order decay. *J. Hydrol.* 49, 213–233.

- 375 [https://doi.org/10.1016/0022-1694\(81\)90214-6](https://doi.org/10.1016/0022-1694(81)90214-6)
- 376 Wagner, D.E., Neupauer, R.M., Cichowitz, C., 2015. Adjoint-based probabilistic source
377 characterization in water-distribution systems with transient flows and imperfect sensors. *J.*
378 *Water Resour. Plan. Manag.* 141, 1–11. [https://doi.org/10.1061/\(ASCE\)WR.1943-5452.0000508](https://doi.org/10.1061/(ASCE)WR.1943-5452.0000508)
- 379 Xing, Z., Qu, R., Zhao, Y., Fu, Q., Ji, Y., Lu, W., 2019. Identifying the release history of a
380 groundwater contaminant source based on an ensemble surrogate model. *J. Hydrol.* 572, 501–
381 516. <https://doi.org/10.1016/j.jhydrol.2019.03.020>
- 382 Zhu, Z., Motta, D., Jackson, P.R., Garcia, M.H., 2017. Numerical modeling of simultaneous tracer
383 release and piscicide treatment for invasive species control in the Chicago Sanitary and Ship
384 Canal, Chicago, Illinois. *Environ. Fluid Mech.* 17, 211–229. [https://doi.org/10.1007/s10652-](https://doi.org/10.1007/s10652-016-9464-1)
385 [016-9464-1](https://doi.org/10.1007/s10652-016-9464-1)
- 386